中國機械工程學刊第四十五卷第二期第 145~159 頁(民國一百一十三年)
Journal of the Chinese Society of Mechanical Engineers, Vol.45, No.2, pp145~159 (2024)

# Injection Molding and Process Parameter Optimization of All-Plastic Front Door Sill Pressure Plate for Automobile

Lu Wang *and Lingfeng Tang *

**Key words:** injection molding process parameters, orthogonal test, EBFNN, NSGA-II.

## ABSTRACT

With the continuous development of plastic strip steel technology, optimization of plastic part process parameters has become one of the hot research in the field of injection molding. This paper takes the automobile front door sill pressure plate as the research object and compares the results of filling time, cavitation, and weld line during the filling process by Moldflow analysis to determine the optimal number and position of gates. Five parameters such as mold temperature and melt temperature were selected as experimental factors, volume shrinkage and warpage are used as evaluation indicators, design of signal-to-noise ratio-based orthogonal tests, determined the optimal combination of process parameters using grey correlation analysis, the results showed that the volume shrinkage and warpage deformation of the two evaluation indexes were reduced by 22.27% and 20.82%, respectively, after optimization. The set of Pareto solutions for volume shrinkage and warping deformation is then obtained by building an Ellipsoidal Basis Function Neural Network (EBFNN) model combined with a Non-dominated Sorting Genetic Algorithm (NSGA-II), the optimum process parameters were determined as mold temperature 40.5°C, melt temperature 221.4°C, injection time 3.9s, packing pressure 54.8 MPa and packing time 39.6s, the maximum volume shrinkage of the optimized part is 5.475%, the warpage deformation is 1.010mm.

*Paper Received March, 2023. Revised July, 2023. Accepted October, 2023. Author for Correspondence: Lu Wang*

**Lu Wang Student, School of Mechanical Engineering, Anhui Polytechnic University, Wuhu, Anhui 241000, China.*

**Lingfeng Tang Professor, School of Mechanical Engineering, Anhui Polytechnic University, Wuhu, Anhui 241000, China.*

## INTRODUCTION

With the rapid development of the economy, the automobile has become a very important means of transportation for the public. The huge industry chain of automobiles has brought wealth to human beings and at the same time caused great pressure on resources and the environment. In order to improve the resources and environmental problems caused by the automotive industry, automotive lightweighting has gradually become one of the hot research in the automotive industry. In this context, experts and scholars have researched a variety of lightweight materials to meet the performance requirements of automotive lightweighting, among which PP composites are gradually being widely used in automotive exterior and interior parts to replace traditional sheet metal parts to achieve weight reduction of automobiles. Injection molding is a typical processing and manufacturing method of automotive plastic parts, various quality problems often occur during the molding process, to improve product quality, the most economical way to improve product quality is to optimize the process parameters when the product structure and mold structure are determined. Optimizing process parameters with CAE technology and intelligent algorithms are of great engineering importance to improve product quality, shorten development cycles and increase product competitiveness.

According to the structural characteristics of sliding door hook plastic parts, Xu Lanying et al. (2022) designed a mold casting system with two cavities and a cooling system and used Moldflow to analyze the mold flow of the injection process, and the simulation results verified the rationality of the mold structure design, which has important reference value for the mold design of the same type of plastic parts. Huang Fengli et al. (2009) proposed an injection molding process parameter optimization method based on integrated correlation, Kriging model, and adaptive genetic-ant colony algorithm for two quality indicators, warpage and shrinkage, in the injection molding process. The results of injection molding process parameter optimization were reliable through mold flow analysis and actual injection molding experiments. In order to improve the molding quality of a thick-walled plastic product, He Shengyan et al. (2015) combined the orthogonal experiment method, studied the influence of each factor on each evaluation index by mean value analysis and extreme difference analysis and obtained a set of optimal process parameters by the comprehensive scoring method. Geng Haizhen et al. (2015) mainly studied the effects of different gate forms and a different number of cavities on the amount of warpage deformation during the injection molding process, which resulted in improved injection efficiency and cost savings. Jyoti Agarwal et al. (2020) studied the development of innovative composite materials to reduce fuel consumption in automobiles and explored the new composite polypropylene (PP) as a major research hotspot and a boon in reducing the consumption of automobiles in terms of lightweighting. Sung-Wook Park et al. (2018) studied the optimization process of the body structure by using a model for multi-objective optimization by reducing the mass as much as possible while ensuring the vehicle performance and derived an optimal solution based on the design objective using an objective programming approach. Vishwanath Panwar et al. (2021) proposed an experimental study of the response surface method and genetic algorithm for optimization of surface roughness of alloy steel turning, combined with Box-Behnken structural matrix for 15 sets of experiments, designed mathematical framework of surface roughness using surface response method of response surface model, and finally optimized this model using a genetic algorithm to obtain the optimum settings of process parameters. The optimal surface roughness response value of 1.19 $\mu m$ was obtained by analyzing the single-objective genetic algorithm optimization. Kuldip Singh Sangwan et al. (2017) studied the optimization of machining process parameters by integrated response surface and genetic algorithm, and established a functional expression between machining process parameters and optimization indexes i.e., a line response surface model based on the experimental results, and tested the correctness of the response surface model with the error controlled within 4%. The response surface model of the optimization index was validated by combining the significance F-value and ANOVA, and finally, the response surface model of the optimization index was optimized by using a genetic algorithm to find the best, thus reducing the energy consumption of the machining process on the machine tool. Heidari Behzad Shiroud et al. (2018) reduced the values of warpage and contraction to 0.287222 mm and 13.6613% by using ANOVA through simulation analysis of important components of the artificial skeletal joint. Saad M. S. Mukras et al. (2019) proposed a framework for determining the optimal injection molding process parameters to minimize product defects through experiment-based multi-objective optimization, considering seven process parameters such as mold temperature and melt temperature, two evaluation indexes such as volume shrinkage and warpage deformation, and the warpage and volume shrinkage of the obtained injection molded experimental products and using these two relationships, a multiobjective problem was proposed to minimize The multi-objective problem of minimizing the two defects is solved using genetic algorithm, and the experimental results show that it is close to the optimization results with a difference of about 7%.

In this paper, mold temperature, melt temperature, injection time, packing pressure, and packing time are selected as experimental factors, and volume shrinkage and warpage deformation are used as evaluation indexes, design orthogonal tests based on signal-to-noise ratio and combine with grey correlation analysis to determine the primary and secondary factors affecting molding quality and the optimal combination of process parameters. Design full-scale experiments and establish sample points with orthogonal test data, the EBFNN model is developed, and the Pareto solution set of volume shrinkage and warpage deformation is obtained by combining NSGA-II multi-objective search algorithm, the optimal process parameters were finally determined, and the optimized volume shrinkage was evenly distributed with a maximum of 5.475% and warpage deformation of 1.010mm. Compared with the maximum volume shrinkage of 9.205% and warpage deformation of 1.739mm under the initial injection process parameters, the molding quality of plastic parts was significantly improved.

## DESIGN OF OPTIMAL POURING SYSTEM FOR AUTOMOBILE FRONT DOOR SILL PRESS PLATE AND SIMULATION STUDY OF ITS INJECTION MOLDING PROCESS

In order to improve the defects of the injection molding process and reduce the production cost, this chapter uses the injection molding software Moldflow to design and optimize the pouring system of the model.

**Pre-processing for Moldflow analysis of automobile front door sill press plate**

Before Moldflow can analyze the injection molding process, it needs to import the model, divide and repair the mesh, then select the material, and set the initial process parameters, etc.

(1) Automobile front door sill pressure plate 3D modeling

3D modeling using CATIA on the basis of the original sheet metal part model, the model of the all- plastic front door sill pressure plate of the car was obtained as shown in Figure 1. The model size is $114mm \times 418mm \times 89mm$, and the average wall thickness is $2.50mm$.

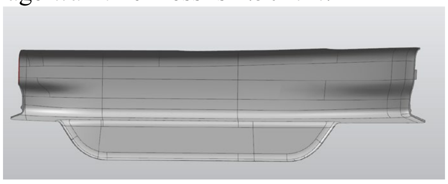

Fig 1. Automobile full plastic front door sill pressure plate model

(2) Mesh type selection and division

The 3D model is converted to igs format and imported into Moldflow for meshing. The purpose of this step is to convert the physical model into a mathematical model. The mesh size and quality have a close relationship with the simulation results and speed, and the mesh size should be set as small as possible to obtain the best simulation results. Moldflow provides three types of meshes: dual- level meshes, 3D meshes, and neutral surface meshes. The automobile front door sill pressure plate is a thin-walled plastic part, usually set the mesh type to dual-level mesh, mesh size is 1.5~2 times the thickness of the part, the average thickness of the model is 2.5 mm, and the edge length of the mesh is set to 4 mm for comprehensive consideration. The mesh quality results are shown in Table 1.

Table 1 Mesh division results table

| Projects | Value |
|---|---|
| Number of meshes | 57650 |
| Mesh matching percentage | 93.2% |
| Mesh mutual percentage | 90.8% |
| Average aspect ratio | 1.88 |
| Minimum aspect ratio | 1.16 |
| Maximum aspect ratio | 17.04 |

In Moldflow numerical simulation analysis, it is generally required that the percentage of dual-level mesh matching and the percentage of mesh mutual is not less than 85%. In order to improve the accuracy of the simulation results, the maximum aspect ratio needs to be controlled within 10. The average aspect ratio is 1.88, and the maximum aspect ratio is 17.04, which is greater than the required maximum aspect, so the grid needs to be repaired.

(3) Mesh repair

Import the model into CAD Doctor for mesh repair, using both automatic and manual repair methods to repair. The automatic repair can only be used as an aid for mesh repair, and manual repair is required to obtain better mesh quality, this includes merging nodes, node matching, local re-gridding, etc. The mesh division of the repaired model is shown in Figure 2, the partial enlargement of the back side is shown in Figure 3, and the division results are shown in Table 2.

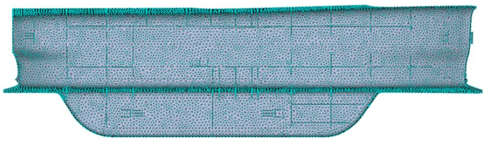

Fig 2. Automobile full plastic front door sill pressure plate model

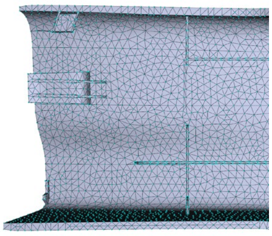

Fig 3. Partial enlargement of the mesh on the back

Table 2 Mesh repair results

| Projects | Value |
|---|---|
| Number of meshes | 57544 |
| Mesh matching percentage | 95.2% |
| Mesh mutual percentage | 94.2% |
| Average aspect ratio | 1.86 |
| Minimum aspect ratio | 1.16 |
| Maximum aspect ratio | 8.86 |

From the restoration results in Table 2, it can be seen that the mesh matching percentage and mesh mutual percentage are greater than 90%, the maximum aspect ratio is reduced to 8.86, which is within the required range, and the mesh quality meets the simulation requirements.

(4) Front door sill pressure plate material setting

The material is PP composite material requested by the customer, the material has excellent heat resistance, stiffness, and strength to meet the requirements of plastic instead of steel, is a comprehensive performance thermoplastic, Specific grade PP+EPDM-T20, is produced by Shanghai PRET Composites Co Ltd, and its viscosity curve and PVT curve are shown in Figures 4 and 5.

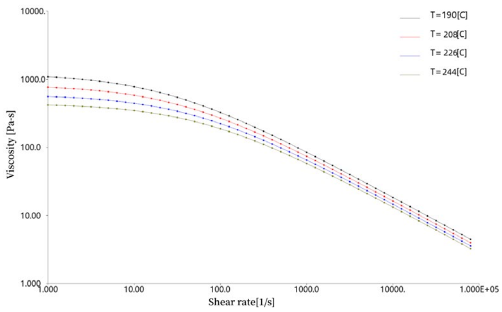


Fig 4. Viscosity curve of the material

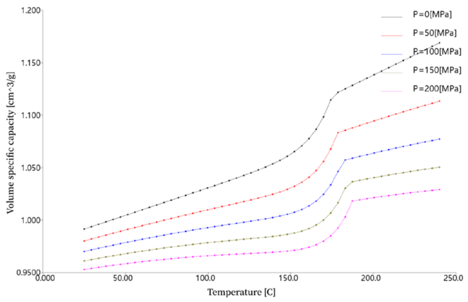


Fig 5. Material PVT curve

The main mechanical property parameters of the material include a modulus of elasticity of 1700 MPa, Poisson's ratio of 0.37, and a shear modulus of 700 MPa.

**Study of automobile front door sill pressure plate pouring system**

The difference in gate location and quantity makes a big difference in the quality of the molded product. The optimal number of gates and gate locations are key factors in ensuring the final molded quality of the product.

(1) Moldflow-based gate location search

In order to choose the right number of gates and gate positions, the "gate position" analysis sequence in Moldflow is used to assist the setting of gate positions. In this paper, the number of gates is set to 1, 2, and 3 respectively according to the actual production experience. The matching cloud diagram of the gate position is shown in Figure 6.

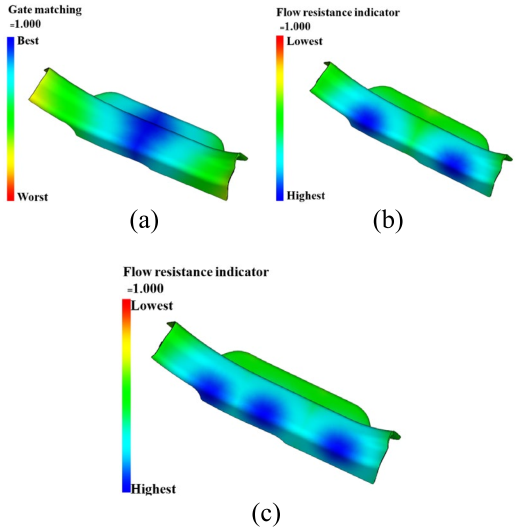


Fig 6. Gating search results

(a) 1 gate matching schematic; (b) 2 gate matching schematic; (c) 3 gate matching schematic

In the cloud diagram of the three options, the blue color indicates the best location for the gate with the least resistance during the filling process, while the red color indicates the most resistance during the filling process. In order to avoid the part will not leave traces on the decorative surface after injection molding, the gate location should be avoided on the decorative surface and set on the side of the part as much as possible. Therefore, Moldflow's gate search results need to be improved.

(2) Pouring system design

The design of the pouring system directly affects the quality, dimensional accuracy, and molding cycle time of the product. As the automobile front door sill pressure plate is a product with high requirements for appearance, there should be no marks on the surface. The pouring system with mixed hot and cold runners is chosen. The main flow channel adopts a hot runner structure, which is conducive to improving the injection pressure and material utilization rate, speeding up the injection speed and ensuring the filling quality of the parts, opening cold runners before entering the cavity, and adopting side gates with trapezoidal gate cross-section, which can improve the quality of product appearance to a certain extent.

The automobile front door sill pressure plate belongs to the left and right parts in the automobile interior parts, so the layout of one mold with two cavities is used for its injection molding, which can improve the production efficiency and save cost, and the obtained pouring system is shown in Figure 7.

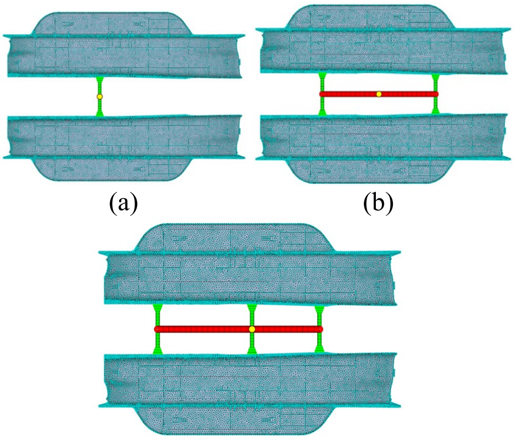
(a) (b)
(c)
Fig 7. Pouring system
(a) 1-gate pouring system; (b) 2-gate pouring system; (c) 3-gate pouring system

(3) Pouring system optimization study

By comparing the results of filling time, volume shrinkage, cavitation, and weld line during the filling process, the number and location of gates can be determined. The simulation of injection molding was done separately for three kinds of pouring systems. The injection process parameters were set as follows: mold temperature 50℃, melt temperature 208℃, injection time 2s, packing pressure 40MPa, packing time 20s, and the analysis result cloud is shown in the figure below.

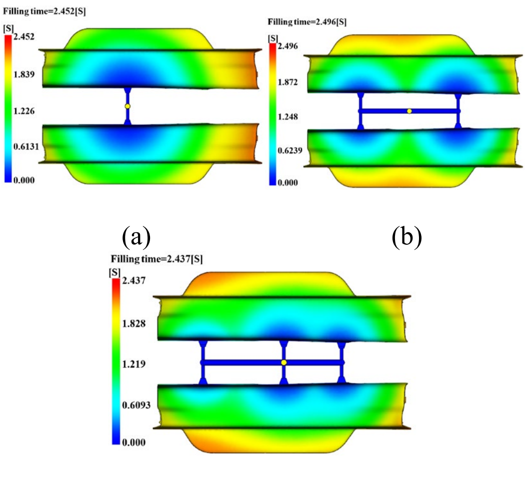

(a) (b)
(c)
Fig 8. Filling time cloud chart
(a) 1-gate pouring system; (b) 2-gate pouring system; (c) 3-gate pouring system

The filling results from Fig. 8 show that the filling times of the three gates are not very different, 2.453s,2.496, and 2.437s, respectively.

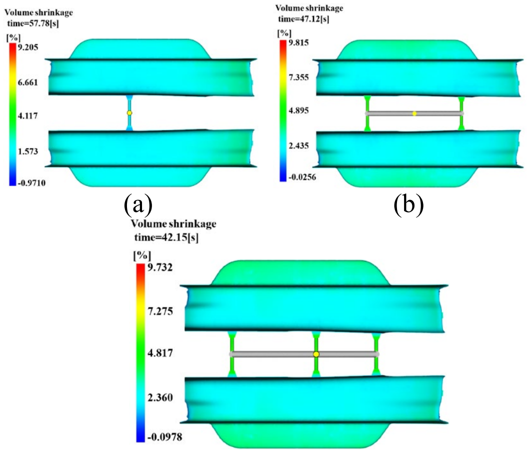

(a) (b)
(c)
Fig 9. Volumetric shrinkage cloud chart
(a) 1-gate pouring system; (b) 2-gate pouring system; (c) 3-gate pouring system

From the volume shrinkage cloud in Figure 9, the volume shrinkage of gate 1 is maximum of 9.205%, that of gate 2 is maximum of 9.815% and that of gate 3 is maximum of 9.732%.

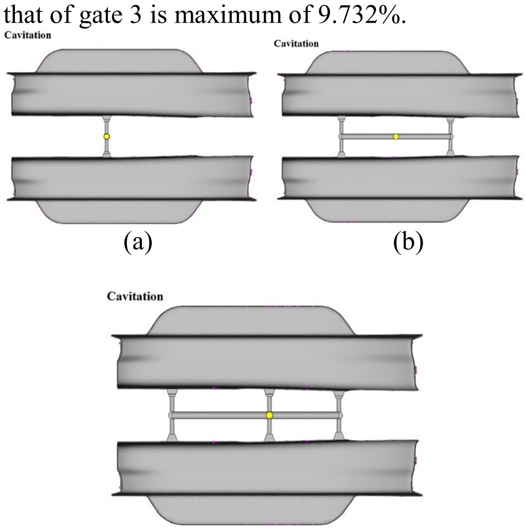

(a) (b)
(c)
Fig 10. Cavitation cloud chart
(a) 1-gate pouring system; (b) 2-gate pouring system; (c) 3-gate pouring system

Cavitations will make the quality and structural stability of the molded part deteriorate, therefore, we need to try to select a pouring system that produces fewer cavitation s for injection molding.

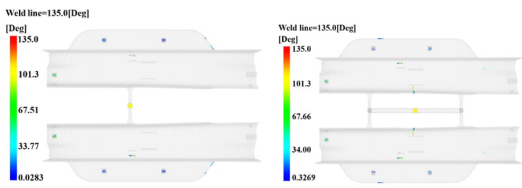

(a) (b)

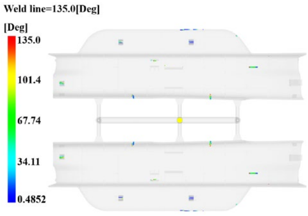


(c)

Fig 11. Weld line cloud chart
(a) 1-gate pouring system; (b) 2-gate pouring system; (c) 3-gate pouring system

The cloud diagram in Fig. 11 shows that the weld line of gate 1 has the best quality. Since the front door sill pressure plate of the car is an exterior part, the quality of the weld line is high.

In summary, the results of filling time, volume shrinkage, cavitation, and weld line are clouded by comparing the three pouring systems, as shown in Table 3.

| Program | Filling time/(s) | Volume shrinkage /(%) | Cavitation /(pcs) | Weld line /(bar) |
|---|---|---|---|---|
| 1 gate | 2.453 | 9.205 | 95 | 25 |
| 2 gates | 2.496 | 9.815 | 85 | 36 |
| 3 gates | 2.437 | 9.732 | 128 | 32 |

By comparing Table 3, it can be concluded that the 1-gate pouring system gives the best results, so 1-gate is chosen as the gating solution for this paper.

## OPTIMIZATION OF INJECTION MOLDING PROCESS PARAMETERS BASED ON ORTHOGONAL TEST

Orthogonal experimental design is an efficient, rapid, and economical experimental design method to study multi-factor and multi-level. In this chapter, the volume shrinkage and warpage deformation of automobile front door sill press plate is taken as process parameter optimization objectives. designing a 5-factor, 4-level orthogonal test based on the signal-to-noise ratio, and transforming the multi-objective problem into a single-objective optimization problem by combining grey correlation analysis, the best combination of process parameters was obtained using extreme difference analysis.

### Design of orthogonal test

The orthogonal test is a widely recognized and highly effective experimental design method with unparalleled advantages for finding the best for complex objectives under the influence of multiple factors. The main use of orthogonal tables for experimental design Each orthogonal table has a code $L_n(m^k)$, where L is the representative symbol of the orthogonal table; n is the number of experiments; m is the number of levels of each selected parameter; and k is the number of parameters.

(1) Orthogonal test factors and evaluation index selection

The thickness of the front door sill platen in this paper is uneven, so it will produce warpage deformation in the process of injection molding, and the volume shrinkage rate of each part of the plastic part is the main cause of its warpage deformation, so the volume shrinkage rate and warpage deformation of the front door sill platen of the car will be used as the test index.

The injection molding process of automobile front door sill pressure plate is influenced by many factors. By reviewing the literature, it is found that, among them, mold temperature, melt temperature, injection time, packing pressure, and packing time are the main factors affecting the volume shrinkage and deformation of the product during the injection molding process. The temperature of the mold is too high, which will cause the mold to stick and also cause bright spots in the local area; when the temperature is too low, the mold will be too tight, which is not conducive to mold exit and easy to strain the plastic parts; the melt temperature needs to be decided according to the temperature characteristics of different materials; too high a melt temperature will cause the material to lose activity and thermal deformation of the machine; the shorter the injection time, the higher the injection rate, and the size of the injection rate has a great impact on the performance of the molded part. Increasing the injection rate will help to reduce the heat loss in mold filling and reduce the shrinkage rate of the product. If the packing pressure is applied properly, the quality defects of the product will be reduced; if the packing time is too short, the shrinkage of the product will be increased and bubbles will be caused, if the packing time is too long, the stress will be generated inside the product and it will be easy to crack, etc. Therefore, the five main factors of mold temperature (A/°C), melt temperature (B/°C), injection time (C/s), packing pressure (D/MPa), and packing time (D/s) were used as test factors.

(2) Establishing an orthogonal test table

The range of levels of the factors is determined based on the range of process parameters recommended for the material in Moldflow. The selected level settings for each factor are shown in Table 4. The 16 groups of orthogonal tests were combined in Moldflow to do injection molding simulation, and the experimental results of each group were obtained as shown in Table 5.

Table 4 Level factor setting

| Level | Factor | | | | |
|---|---|---|---|---|---|
| | A | B | C | D | E |
| 1 | 40 | 190 | 1 | 40 | 10 |
| 2 | 50 | 208 | 2 | 45 | 20 |
| 3 | 60 | 226 | 3 | 50 | 30 |
| 4 | 70 | 244 | 4 | 55 | 40 |

Table 5 Orthogonal test scheme and results

| No | A | B | C | D | E | Volume shrinkage | Warpage |
|---|---|---|---|---|---|---|---|
| 1 | 40 | 190 | 1 | 40 | 10 | 9.229 | 1.867 |
| 2 | 40 | 208 | 2 | 45 | 20 | 7.534 | 1.593 |
| 3 | 40 | 226 | 3 | 50 | 30 | 9.706 | 1.312 |
| 4 | 40 | 244 | 4 | 55 | 40 | 9.316 | 1.037 |
| 5 | 50 | 190 | 2 | 50 | 40 | 5.966 | 1.599 |
| 6 | 50 | 208 | 1 | 55 | 30 | 8.446 | 1.434 |
| 7 | 50 | 226 | 4 | 40 | 20 | 9.227 | 1.479 |
| 8 | 50 | 244 | 3 | 45 | 10 | 12.11 | 1.705 |
| 9 | 60 | 190 | 3 | 55 | 20 | 6.995 | 1.422 |
| 10 | 60 | 208 | 4 | 50 | 10 | 10.23 | 1.372 |
| 11 | 60 | 226 | 1 | 45 | 40 | 9.008 | 1.596 |
| 12 | 60 | 244 | 2 | 40 | 30 | 8.977 | 1.558 |
| 13 | 70 | 190 | 4 | 45 | 30 | 7.641 | 1.634 |
| 14 | 70 | 208 | 3 | 40 | 40 | 8.565 | 1.726 |
| 15 | 70 | 226 | 2 | 55 | 10 | 10.03 | 2.333 |
| 16 | 70 | 244 | 1 | 50 | 20 | 11.15 | 1.406 |

(3) Signal-to-noise ratio

The ratio of signal power and noise is called the signal-to-noise ratio, which is often used to measure the degree of influence of various factors on the results and can be used as a basis for judging the stability of the experiment. The signal-to-noise ratio is divided in different situations into nominal- the-best characteristic, larger-the-better characteristic, and smaller-the-better characteristic. In order to improve the molding quality of the automobile front door sill press plate, the evaluation index selected in this paper should be as small as possible, so the smaller-the-better characteristic is chosen. Its signal-to-noise ratio is calculated by the formula.

$$S/N = -10\lg\left(\frac{1}{n}\sum_{i=1}^{n} x_i^2\right) \qquad (1)$$

Where: $S/N$—Signal-to-noise ratio (dB);

$x_i$—the value of the i-th experiment;

n—number of repetitions of the experiment.

The signal-to-noise ratio is calculated by substituting the volume shrinkage and warpage deformation data into equation (1), and the results are shown in Table 6.

Table 6 S/N results of orthogonal test

| No | Volume shrinkage | S/N /(dB) | Warpage | S/N /(dB) |
|---|---|---|---|---|
| 1 | 9.229 | -19.30 | 1.867 | -5.42 |
| 2 | 7.534 | -17.54 | 1.593 | -4.04 |
| 3 | 9.706 | -19.74 | 1.312 | -2.36 |
| 4 | 9.316 | -19.38 | 1.037 | -0.32 |
| 5 | 5.966 | -15.51 | 1.599 | -4.08 |
| 6 | 8.446 | -18.53 | 1.434 | -3.13 |
| 7 | 9.227 | -19.30 | 1.479 | -3.40 |
| 8 | 12.11 | -21.66 | 1.705 | -4.63 |
| 9 | 6.995 | -16.90 | 1.422 | -3.06 |
| 10 | 10.23 | -20.20 | 1.372 | -2.75 |
| 11 | 9.008 | -19.09 | 1.596 | -4.06 |
| 12 | 8.977 | -19.06 | 1.558 | -3.58 |
| 13 | 7.641 | -17.66 | 1.634 | -4.27 |
| 14 | 8.565 | -18.65 | 1.726 | -4.74 |
| 15 | 10.03 | -20.03 | 2.333 | -7.36 |
| 16 | 11.15 | -20.95 | 1.406 | -2.96 |

## Gray correlation analysis

Gray correlation analysis is applicable to multi-objective optimization problems with small sample sizes. By establishing the relationship between the signal-to-noise ratio data and the ideal value of the evaluation index after dimensionless processing, calculating the gray correlation, and extreme difference analysis, the multi-objective optimization problem is converted into a single-objective optimization problem to obtain the optimal combination of injection molding process parameters for automobile front door sill press plate.

(1) Gray correlation calculation

In order to eliminate the effect of odd sample data on the results, the signal-to-noise ratio needs to be dimensionless, and the dimensionless formula is as follows:

$$y_i = \frac{a_{i\ max} - a_i}{a_{i\ max} - a_{i\ min}} \qquad (2)$$

Where: $a_i$—Signal-to-noise ratio of the i-th experiment evaluation index;

$a_{i\ max}$—maximum signal-to-noise ratio of each evaluation index;

$a_{i\ min}$—minimum signal-to-noise ratio of each evaluation index;

$y_i$ —signal-to-noise ratio value after dimensionless.

The degree of correlation between the dimensionless S/N data and the ideal value is called the gray correlation coefficient and is calculated as:

$$\delta_i = \frac{|y_i^0 - y_i|_{min} + \rho|y_i^0 - y_i|_{max}}{|y_i^0 - y_i| + \rho|y_i^0 - y_i|_{max}} \quad (3)$$

Where: $\delta_i$—Grey incidence coefficient;

$y_i^0$—the ideal value of the i-th experimental data, generally taken as 0;

$\rho$ —the resolution factor, $\rho \in [0,1]$ , is generally taken as 0.5.

The average of the gray correlation coefficients of the evaluation indicators is called the gray correlation degree, and the larger the value of the gray correlation degree, the greater the convergence of the experimental evaluation indicators under the influence of various factors. The gray correlation was calculated according to equation (4), and the analysis results are shown in Table 7, where dimensionless values are denoted by $D_{SS}$, gray incidence coefficients are denoted by $G_{ic}$, and gray correlations are denoted by $G_{cd}$.

$$\gamma_i = \frac{1}{m}\sum_{i=1}^{n} \delta_i \quad (4)$$

Where: $\gamma_i$—grey correlation degree;

m—optimize the number of targets, m is taken as 2.

Table 7 Results of gray correlation analysis

| No | Volume shrinkage | | | Warpage | | | $G_{cd}$ |
|---|---|---|---|---|---|---|---|
| | S/N | $D_{SS}$ | $G_{ic}$ | S/N | $D_{SS}$ | $G_{ic}$ | |
| 1 | -19.30 | 0.62 | 0.45 | -5.42 | 0.72 | 0.41 | 0.43 |
| 2 | -17.54 | 0.33 | 0.60 | -4.04 | 0.53 | 0.49 | 0.55 |
| 3 | -19.74 | 0.69 | 0.42 | -2.36 | 0.29 | 0.63 | 0.53 |
| 4 | -19.38 | 0.63 | 0.44 | -0.32 | 0.00 | 1.00 | 0.72 |
| 5 | -15.51 | 0.00 | 1.00 | -4.08 | 0.53 | 0.49 | 0.75 |
| 6 | -18.53 | 0.49 | 0.51 | -3.13 | 0.40 | 0.56 | 0.54 |
| 7 | -19.30 | 0.62 | 0.45 | -3.40 | 0.44 | 0.53 | 0.49 |
| 8 | -21.66 | 1.00 | 0.33 | -4.63 | 0.61 | 0.45 | 0.39 |
| 9 | -16.90 | 0.23 | 0.69 | -3.06 | 0.39 | 0.56 | 0.63 |
| 10 | -20.20 | 0.76 | 0.40 | -2.75 | 0.35 | 0.59 | 0.50 |
| 11 | -19.09 | 0.58 | 0.46 | -4.06 | 0.53 | 0.49 | 0.48 |
| 12 | -19.06 | 0.58 | 0.46 | -3.58 | 0.50 | 0.50 | 0.48 |
| 13 | -17.66 | 0.35 | 0.59 | -4.27 | 0.56 | 0.47 | 0.53 |
| 14 | -18.65 | 0.51 | 0.50 | -4.74 | 0.63 | 0.44 | 0.47 |
| 15 | -20.03 | 0.73 | 0.41 | -7.36 | 1.00 | 0.33 | 0.37 |
| 16 | -20.95 | 0.88 | 0.36 | -2.96 | 0.38 | 0.57 | 0.47 |

(2) Analysis of the extreme difference

In order to obtain the degree of influence of each factor on the evaluation index and the best combination of injection molding process parameters, it is necessary to calculate the mean and extreme difference values of gray correlation degree under different combinations of process parameters. The difference between the maximum value and the minimum value in a group of data is called the extreme difference, and the larger the extreme difference is, the greater the influence of the factor on the evaluation index. The calculation results are shown in Table 8.

Table 8 Extreme difference analysis of gray correlation

| Projects | Factor | | | | |
|---|---|---|---|---|---|
| | A | B | C | D | E |
| Mean value 1 | 0.558 | 0.585 | 0.480 | 0.468 | 0.423 |
| Mean value 2 | 0.543 | 0.515 | 0.538 | 0.488 | 0.535 |
| Mean value 3 | 0.523 | 0.468 | 0.505 | 0.563 | 0.520 |
| Mean value 4 | 0.460 | 0.515 | 0.560 | 0.565 | 0.605 |
| Extreme difference | 0.098 | 0.117 | 0.080 | 0.097 | 0.182 |

From the calculation results of each factor in Table 9, it can be seen that the combined influence of each process parameter on the volume shrinkage and warpage deformation of the front door sill platen is, in descending order, as follows: mold temperature, mold temperature, injection time, packing pressure and packing time. The optimal combination of process parameters is $A_1B_1C_4D_4E_4$, that is, mold temperature 40 °C, melt temperature 190 °C, injection time 4s, and packing pressure 55 MPa, packing time 40s.

(3) Optimization result verification

The optimal injection molding process parameters were obtained by combining signal-to-noise ratio and gray correlation analysis for the automobile front door sill platen optimized by the method, further verification of the accuracy of the described method is required, and the best combination of process parameters $A_1B_1C_4D_4E_4$ obtained is experimentally verified, as shown in Figures 12 and 13.

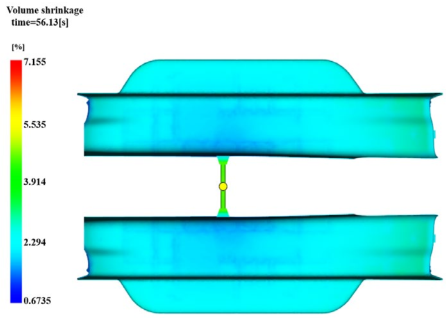

Fig 12. Volume shrinkage

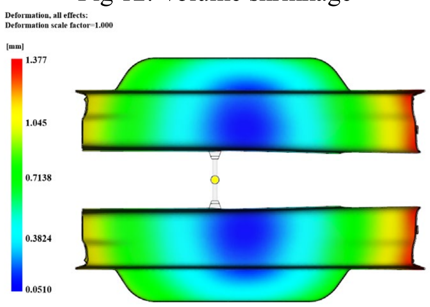

Fig 13. Warpage

The volume shrinkage of the optimized part was 7.155%; the warpage deformation was 1.377 mm. Compared with the volume shrinkage of 9.205% and warpage deformation of 1.739 mm under the initial injection molding process parameters, it can be seen that the volume shrinkage and warpage deformation of the two evaluation indexes were reduced by 22.27% and 20.82%, respectively, after optimization. The quality of the molded parts is improved, and the feasibility and effectiveness of the optimization method combining the signal-to-noise ratio-based orthogonal test and gray correlation analysis are verified.

## PROCESS PARAMETER OPTIMIZATION BASED ON ELLIPSOIDAL BASIS FUNCTION NEURAL NETWORK AND NON-DOMINATED SORTING GENETIC ALGORITHM

The 16 sets of data obtained from orthogonal experiments cannot include all the values between the minimum and maximum levels of each process parameter, and the method can only obtain the local optimal process parameters, but not the global optimal process parameters. In this chapter, an Ellipsoidal Basis Function Neural Network (EBFNN) model with input as process parameters and output as evaluation indexes will be built, and the process parameters corresponding to the optimal evaluation index will be predicted in conjunction with Non-dominated Sorting Genetic Algorithm (NSGA-II).

### Sample data selection

The selection of sample data plays a critical role in the accuracy of building the EBFNN model. Theoretically, the more sample data are selected, the more accurately the neural network is trained to simulate the system. In order to obtain more accurate optimization results, a comprehensive design of the experiment is also required. Three levels were taken for each factor, and the specific level values are shown in Table 9, and a total of 243 sets of experimental data were obtained. The sample points and results are shown in Table 11, and the data in the last 16 rows of Table 10 are from the orthogonal test.

Table 9 Table of the levels of each factor in the full-scale test

| Level | A | B | C | D | E |
|---|---|---|---|---|---|
| 1 | 40 | 190 | 1 | 40 | 10 |
| 2 | 55 | 217 | 2.5 | 47.5 | 25 |
| 3 | 70 | 244 | 4 | 55 | 40 |

Table 10 Sample points and results

| No | A | B | C | D | E | Volume shrinkage | Warpage |
|---|---|---|---|---|---|---|---|
| 1 | 40 | 190 | 1 | 40 | 10 | 9.229 | 1.867 |
| 2 | 40 | 190 | 1 | 40 | 25 | 7.325 | 1.913 |
| 3 | 40 | 190 | 1 | 40 | 40 | 6.383 | 1.913 |
| 4 | 40 | 190 | 1 | 47.5 | 10 | 9.154 | 1.684 |
| 5 | 40 | 190 | 1 | 47.5 | 25 | 7.066 | 1.734 |
| 6 | 40 | 190 | 1 | 47.5 | 40 | 5.908 | 1.734 |
| 7 | 40 | 190 | 1 | 55 | 10 | 9.084 | 1.498 |
| 8 | 40 | 190 | 1 | 55 | 25 | 6.660 | 1.543 |
| 9 | 40 | 190 | 1 | 55 | 40 | 5.514 | 1.543 |
| 10 | 40 | 190 | 2.5 | 40 | 10 | 9.088 | 1.760 |
| … | … | … | … | … | … | … | … |
| 243 | 70 | 244 | 4 | 55 | 40 | 9.273 | 1.172 |
| 244 | 40 | 190 | 1 | 40 | 10 | 9.229 | 1.867 |
| 245 | 40 | 208 | 2 | 45 | 20 | 7.534 | 1.593 |
| 246 | 40 | 226 | 3 | 50 | 30 | 9.706 | 1.312 |
| 247 | 40 | 244 | 4 | 55 | 40 | 9.316 | 1.037 |
| 248 | 50 | 190 | 2 | 50 | 40 | 5.966 | 1.599 |
| … | … | … | … | … | … | … | … |
| 259 | 70 | 244 | 1 | 50 | 20 | 11.15 | 1.406 |

**EBFNN model building**

In order to obtain the global optimal solution, it is necessary to re-optimize the injection molding process parameters. In this section, the mold temperature, melt temperature, injection time, packing pressure, and packing time are used as inputs, and the volume shrinkage and warpage deformation are used as outputs to build the EBFNN approximation model using Isight.

(1) Mathematical model for multi-objective optimization problems

Without loss of generality, the minimization problem for the multi-objective optimization problem can be expressed in the following mathematical form:

$$\begin{cases} Minimize: f(x) = \{f_1(x), f_2(x), \ldots, f_k(x)\} \\ subject\ \ to: g(x) \le 0; p = 1,2,\ldots,l \\ h(x) = 0; q = 1,2,\ldots,m \\ x = [x_1, x_2, \ldots, x_n]^T \\ x_{iu} \le x_i \le x_{id}, i = 1,2,\ldots,n \end{cases} \tag{5}$$

Where: $f(x)$—Objective function;

$g(x)$—inequality constraint function;

$h(x)$—equation constraint function;

$n$ —optimize the number of design variables;

$x$—design Variables;

$k$—number of objective functions;

$l$ —number of inequality constraint functions;

$m$ —number of equation constraint functions;

$x_{iu}, x_{id}$—upper and lower limits of design variables.

(2) Ellipsoidal Basis Function Neural Network (EBFNN) overview

In recent years, BP neural network and RBF neural network have achieved a more mature theoretical basis and corresponding application results under the research of domestic and foreign scholars. In view of the characteristics of BP neural networks and RBF neural networks, Kavuri et al. proposed a neural network model with ellipsoidal basis functions, namely Ellipsoidal Basis Function Neural Network (EBFNN). The EBFNN structure is the same as the RBF neural network structure, which is also a feed-forward network model formed by three layers: the input layer, the hidden layer, and the output layer, and can be seen as an extension of the RBF neural network model. Its difference in network structure from BP and RBF neural networks mainly lies in the use of the ellipsoidal unit function for its hidden layer nodes and the use of full covariance matrix instead of diagonal covariance matrix in RBF neural networks, the input space is divided by ellipsoidal morphology, and the function output value is derived from the distance of the input sample data from the center of the ellipse and the axis distance of the ellipsoid, which can divide the input space more precisely and can improve the classification ability of the network. Thus, EBFNN should theoretically have stronger pattern recognition capability than the unbounded RBF neural network. The EBFNN structure is given in Figure 14.

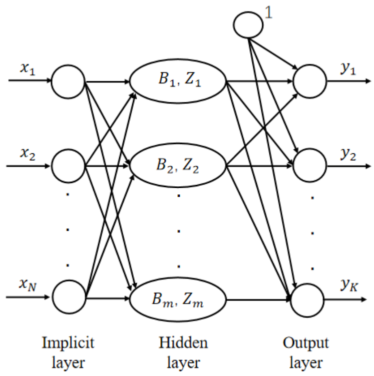


Fig 14. EBFNN structure

An N-dimensional input sample: $x = (x_1, x_2, \ldots, x_n)^T$ and $x \in R^N$, then it is directly input into each hidden node so that the mth EBF node function expression of the hidden layer is:

$$F_m(x) = exp\left\{-\frac{1}{2}(x - B_m)^T Z_m^{-1}(x - B_m)\right\} \tag{6}$$

Where: $B_m$ —Hidden node centroids, $B_m = (B_{1m}, B_{2m}, \ldots, x_{mN}) \in R^N$;

$Z_m$ —full covariance matrix, $Z_m = (\sigma_{st})_{s,t=1}^N$.

The expression of the function of the i-th node of the output layer with respect to x is:

$$G_i(x) = \sum_{m=1}^{M} \alpha_{im}\varphi_m + \alpha_{i0} \tag{7}$$

Where: $\alpha_{im}$ —Connecting the weight of the mth EBF node and the i-th output node;

$\alpha_{i0}$—deviation term of the i-th indicator, $i = 1,2,\ldots,k$.

(3) EBFNN model building and accuracy evaluation

Approximate models are a set of methods that represent the response relationship between inputs and outputs as an approximate mathematical model, which can be used as an alternative to time-consuming and computationally expensive simulations. In this chapter, the EBF neural network approximation model is constructed using the optimization design software Isight. In the main interface Approximation component, select RBF Model as the function approximation technique; in the Date file interface, select the sample type as Sampling Points, and import the first 229 groups of data in Table 11 as the training sample point data. Scan the training sample data in Parameter and define the input variables as the above five process parameters and the output responses as volume shrinkage and warpage, in the Technique Option interface, select Elliptical as the function type, where Smoothing Filter and Maximum lterations to Fit are set to default values. The final error analysis method selected Separate Date File and imported the last 30 sets of sample data in Table 11 for error analysis. where the complex correlation coefficient($R^2$) is calculated as:

$$R^2 = 1 - \frac{\sum_{i=1}^{n}(y_i - \hat{y}_i)^2}{\sum_{i=1}^{n}(y_i - \bar{y}_i)^2} \qquad (8)$$

Where: $n$—Number of samples tested;

$y_i$—numerical simulation of real values;

$\hat{y}_i$—estimated values of the approximate model;

$\bar{y}_i$—true Average.

The results of the error analysis for each output response are shown in Table 11.

Table 11 Model fitting accuracy

| Output Response | $f_{AMAE}$ | $f_{MAE}$ | $f_{RMSE}$ | $R^2$ |
|---|---|---|---|---|
| Volume shrinkage | 0.02855 | 0.19667 | 0.05404 | 0.94053 |
| Warpage | 0.02192 | 0.19741 | 0.04668 | 0.96340 |

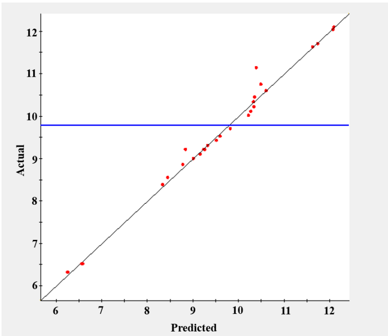


(a)

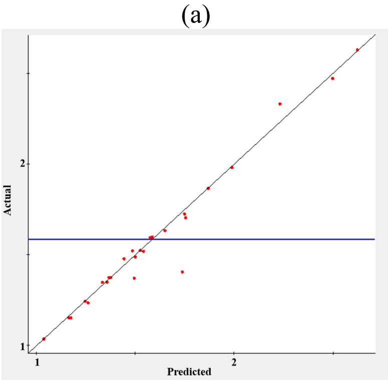


(b)

Fig 15. Model error analysis
(a) Volume shrinkage; (b) Warpage

Among them, $f_{AMAE}$, $f_{MAE}$, and $f_{RMSE}$ are all less than 0.2, and $R^2$ are all greater than 0.9, which indicates that this model is significant, and the relationship between the true and ideal values can be seen in Figure 15, uniformly distributed on both sides of the ideal straight line, which proves that the accuracy of the approximation model meets the requirements and can fit the response values under the combination of different factors.

## NSGA-II based multi-objective injection molding process parameter optimization

In order to quickly find the optimal combination of injection molding process parameters and reduce software simulation and labor costs, the NSGA-II multi-objective optimization algorithm is introduced to find the optimal solution based on the EBFNN model established in the previous section.

(1) Overview of NSGA-II multi-objective optimization algorithm

Genetic algorithms are modeled after the evolutionary phenomenon of biological superiority and inferiority, whose specific phenomena include heredity, mutation, natural selection, and hybridization. It is commonly used in optimization engineering problems, where iterative methods are used to find the optimal solution or solution set from a new population. Goldberg first proposed the concept of the Pareto optimal solution set. The phenomenon of conflicting sub-objectives often occurs in multi-objective optimization, which also requires balanced optimization of sub-objectives to find the Pareto optimal solution set and Pareto frontier. Based on the nondominated genetic algorithm (NSGA) combined with elite strategy and optimal retention strategy, Deb et al. proposed the non-dominated sorting genetic algorithm (NSGA-II) to obtain uniformly distributed noninferior Pareto solutions, NSGA-II not only improves the computational efficiency compared with NSGA algorithm but also solves the optimization problem with constraints. Therefore, this algorithm is chosen as the multi-objective optimization algorithm for process parameters in this chapter.

(2) Multi-objective optimization model building based on EBFNN

The Optimization component is invoked in the multi-objective optimization software Isight to solve the multi-objective optimization of the volume shrinkage and warpage deformation of the injection molding process of the automobile front door sill press plate in combination with the EBF neural network model. The NSGA-II multi-objective optimization algorithm is selected in the interface, and the settings are set to set the population size to 48, the evolutionary generation to 30, the crossover probability to 0.8, and the crossover distribution index and variance distribution index to default values. The design variables and objective function are defined.

(3) Analysis of optimization results

The iterative history of each optimization index obtained by Isight optimization is shown in Figure 16, and the distribution of Pareto solutions of the optimization index is shown in Figure 17.

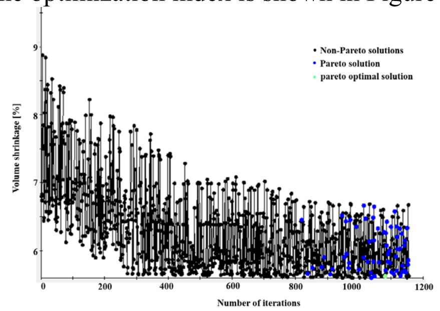


(a)

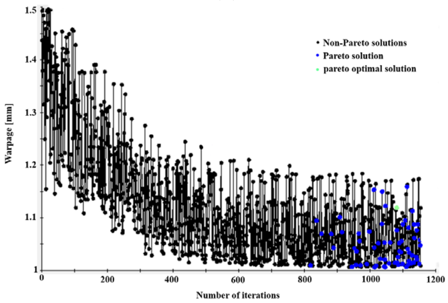


(b)

Fig 16. Iterative evolutionary process
(a) Volume shrinkage; (b) Warpage

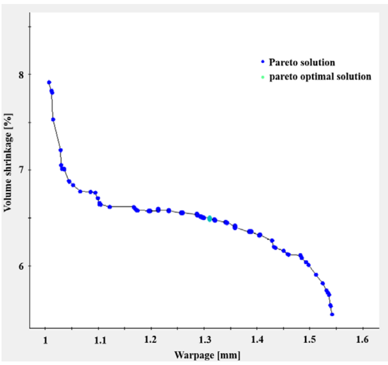


Fig 17. Pareto solution distribution and optimal solution

After 1201 iterations of the algorithm, the Pareto fronts for volume shrinkage and warpage deformation were obtained, and the iterative evolution process is shown in Figure 16. The optimal solution is obtained, and the corresponding optimal process parameters are: mold temperature 40.5°C, melt temperature 221.4°C, injection time 3.9s, packing pressure 54.8 MPa, and packing time 39.6s. The molding quality results are shown in Fig.

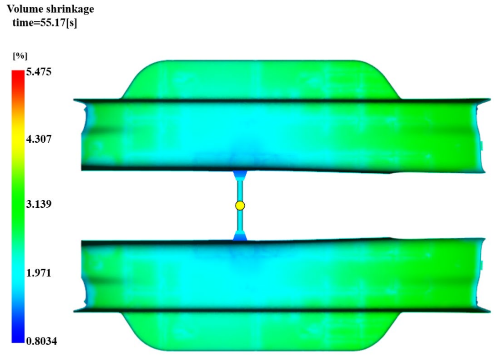


Fig 18. Volume shrinkage

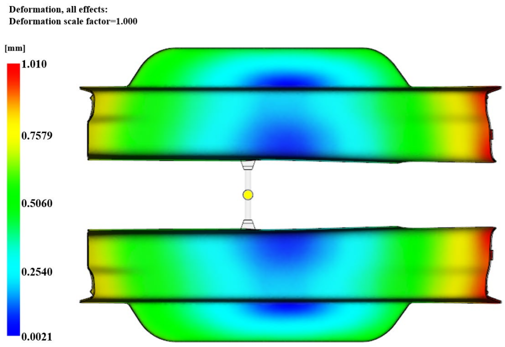


Fig 19. Warpage

The maximum volume shrinkage and warpage deformation of the optimized plastic parts are significantly improved, and the optimized volume shrinkage is evenly distributed with a maximum of 5.475% and warpage deformation of 1.010 mm. Compared with the maximum volume shrinkage of 7.155% and warpage deformation of 1.377 mm optimized by the combination of signal-to-noise ratio-based orthogonal test and gray correlation analysis, the volume shrinkage and warpage deformation were reduced by 23.48% and 26.65%, respectively, and the forming quality of the parts was improved.

## CONCLUSIONS

The 3D data model of the front door sill pressure plate of the automobile was drawn by CATIA on the basis of the original sheet metal parts, and the mesh was repaired in CAD Doctor, three types of pouring systems, one gate, two gates and, three gates, have been created for the front door sill pressure plate. By evaluating the filling time, volume shrinkage, cavitation, and weld line of the three gating systems, the 1 gate gating system is determined to be the best gating system.

According to the influence of process parameters on the molding quality of plastic parts, mold temperature, melt temperature, injection time, packing pressure, and packing time were selected as experimental factors, and volume shrinkage and warpage deformation were used as evaluation indexes to establish a 5-factor, 4-level orthogonal test, the optimal combination of process parameters is $A_1B_1C_4D_4E_4$, i.e. mold temperature 40 ℃, melt temperature 190 ℃, injection time 4 s, packing pressure 55 MPa and packing time 40 s. After optimization, the volume shrinkage is 7.155%; warpage deformation is 1.377 mm. Compared with the initial parameters, the two evaluation indexes of volume shrinkage and warpage deformation are reduced by the volume shrinkage and warpage were reduced by 22.27% and 20.82%, respectively.

Design and complete a comprehensive test to obtain more comprehensive sample point data, establish an EBFNN model combined with NSGA-II multi-objective optimization search algorithm, obtain Pareto solution sets for volume shrinkage and warpage deformation through genetic iteration, the final selection of process parameters was 40.5°C mold temperature, 221.4°C melt temperature, 3.9s injection time, 54.8 MPa packing pressure and 39.6s packing time as the optimal combination. the optimized volume shrinkage is uniformly distributed with a maximum of 5.475%, warpage deformation is 1.010 mm, and the molding quality of the fabricated parts is improved.

## AUTHOR CONTRIBUTIONS

Lu Wang had made substantial contributions to design, experimental research, data collection and result analysis; Lingfeng Tang made critical changes to important academic content;

## DATA AVAILABILITY

The data used to support the findings of this study are included within the article.

## CONFLICTS OF INTEREST

The authors declare that they have no conflicts of interest to report regarding the present study.

## REFERENCES

Pan, Q.Z., ang Zhao, C.G. "Research on Lightweight Brake Structure Based on Equal Strength Design," Railway Locomotive & Vehicle, Vol. 41, No. 05, pp. 65-69 (2021).

Yang, K., Tang, L.F., and Wu, P., "Research on Optimization of Injection Molding Process Parameters of Automobile Plastic Front-End Frame," Advances in Materials Science and Engineering (2022).

Xu, L.Y., Feng, S.C., and Ye, G.S. "Design of Injection Mold for Sliding Door Hook Based on Moldflow," Journal of Guangdong Normal University of Technology, Vol. 43, No. 03, pp. 8-14 (2022).

Huang, F.G., Xu, J.H., and Gu, J.M., "Multi-objective optimization study of injection molding process parameters based on integrated correlation degree," China Plastics, Vol. 23, No. 12, pp.60-64 (2009).

He, S.Y., Chu, C.P., and Deng, J., "CAE-based optimization of injection molding process parameters for thick-walled plastic parts," China Plastics, Vol. 30, No. 12, pp.58-62 (2016).

Geng, H.Z., and Jia, L.L., "Influence Analysis of Cavity Number and gate Position on Deformation Based on Moldflow, " Machinery Manufacturing, Vol. 50, No. 06, pp.76-78 (2015).

Jyoti, A., Swarnalata, S., and Smita, M., "Progress of novel techniques for lightweight automobile applications through innovative eco-friendly composite materials: A review," Journal of Thermoplastic Composite Materials, Vol. 33, No. 7, pp.978-1013 (2020).

Sung, W.P., Jae, H.C., and Byung, C.L., "Multi-objective optimization of an automotive body component with fiber-reinforced composites," Structural and Multidisciplinary Optimization, Vol. 58, No. 5, pp.2203-2217 (2018).

Panwar, V., and Kumar, S.D., "Experimental investigations and optimization of surface roughness in turning of en 36 alloy steel using response surface methodology and genetic algorithm," Materials Today: Proceedings, Vol. 46, No. 15, pp.6474-6481 (2021).

Kuldip, S.S., and Girish, K., "Optimization of Machining Parameters for Improving Energy Efficiency using Integrated Response Surface Methodology and Genetic Algorithm Approach," Procedia CIRP, Vol. 61, pp.517-522 (2017).

Behzad, S.H., Seyed, M.D., and Amin, H.M., "Optimization simulated injection molding process for ultrahigh molecular weight polyethylene nanocomposite hip liner using response surface methodology and simulation of mechanical behavior," Journal of the Mechanical Behavior of Biomedical Materials, Vol. 81, pp.95-105 (2018).

Saad, M.S.M., and Hanafy, M.O., "Experimental-Based Multi-objective Optimization of Injection Molding Process Parameters," Arabian Journal for Science and Engineering, Vol. 44, No. 9, pp.7653-7665 (2019).

Yang, X.F., "Simulation of Injection Molding Process and Optimization of Process Parameters Based on Moldflow," Xiangtan University, China, (2015).

Wang, C., "Study on Injection Molding of polypropylene (PP) based wood plastic Composite," Beijing University of Chemical Technology, China, (2009).

Yan, Z.X., Miao, Y., and Shu, H.T., "Multi-objective optimization of injection molding process Parameters based on signal-to-noise ratio and grey correlation analysis," Chinese Journal of Synthetic Resins and Plastics, Vol. 38, No. 02, pp.54-57+61 (2021).

Yuan, B., and Li, H., "Optimization of barrel-shaped parts thinning and drawing process parameters based on gray correlation degree," Forging and pressing technology, Vol. 44, No. 5, pp.69-73 (2019).

Liu, F., "Multi-objective optimization of automotive front cover injection molding process parameters and its stiffness analysis," Zhongnan University of Forestry Science and Technology, China, (2019).

Deng, F., and Guo, W., " Multi-objective Optimization of microcellular foaming process Parameters based on PSOBPNN and NSGA-Ⅱ," Plastics Industry, Vol. 47, No. 11, pp.49-54-77 (2019).

Xiao, D., and Hu, S.S., "An ellipsoidal basis function neural network based on Rough K-means," Journal of Nanjing University of Aeronautics and Astronautics," pp.321-325 (2006).

Lu, Y.S., and L, He., "Multi-objective Optimization of Injection Process Parameters Based on EBFNN and NSGA-II," Journal of physics. Conference series, Vol. 1637, No. 1, (2020).

Yu, S.H., He, X.M, and Zhang, G.Y., "Injection Molding Process Optimization Based on Response Surface Model and NSGA-Ⅱ Algorithm," Journal of Plasticity Engineering, Vol. 21, No. 03, pp.15-19+141 (2014).

## NOMENCLATURE

$S/N$—Signal-to-noise ratio (dB);

$x_i$—the value of the i-th experiment;

n—number of repetitions of the experiment.

$a_i$ —Signal-to-noise ratio of the i-th experiment evaluation index;

$a_{i\ max}$—maximum signal-to-noise ratio of each evaluation index;

$a_{i\ min}$—minimum signal-to-noise ratio of each evaluation index;

$y_i$ —signal-to-noise ratio value after dimensionless.

Where: $\delta_i$—Grey incidence coefficient;

$y_i^0$—the ideal value of the i-th experimental data, generally taken as 0;

$\rho$ —the resolution factor, $\rho \in [0,1]$, is generally taken as 0.5.

$\gamma_i$—grey correlation degree;

m—optimize the number of targets, m is taken as 2.

$f(x)$—Objective function;

$g(x)$—inequality constraint function;

$h(x)$—equation constraint function;

$n$ —optimize the number of design variables;

$x$—design Variables;

$k$—number of objective functions;

$l$ —number of inequality constraint functions;

$m$ —number of equation constraint functions;

$x_{iu}, x_{id}$—upper and lower limits of design variables.

$B_m$ —Hidden node centroids, $B_m = (B_{1m}, B_{2m}, \dots, x_{mN}) \in R^N$;

$Z_m$ —full covariance matrix, $Z_m = (\sigma_{st})_{s,t=1}^{N}$.

The expression of the function of the i-th node of the output layer with respect to x is:

$$G_i(x) = \sum_{m=1}^{M} \alpha_{im}\varphi_m + \alpha_{i0} \quad (7)$$

$\alpha_{im}$—Connecting the weight of the mth EBF node and the i-th output node;

$\alpha_{i0}$—deviation term of the i-th indicator, $i = 1,2,\dots,k$.

$\alpha_{im}$—Connecting the weight of the mth EBF node and the i-th output node;

$\alpha_{i0}$—deviation term of the i-th indicator, $i = 1,2,\dots,k$.

$n$—Number of samples tested;

$y_i$—numerical simulation of real values;

$\hat{y}_i$—estimated values of the approximate model;

$\bar{y}_i$—true Average.

# 汽車全塑前門檻壓板注塑成型及工藝參數優化研究

王魯 唐鈴鳳

安徽工程大學機械工程學院

### 摘要

摘要：隨著塑帶鋼技術的不斷發展，塑件工藝參數優化已經成為注塑成型領域的熱點研究之一，本文以汽車前門檻壓板為研究物件，

通過 Moldflow 分析對比充填過程中的充填時間、氣穴和熔接線等結果，確定最佳的澆口數量和位置。選取模具溫度、熔體溫度等五個參數作為主要實驗因素，以體積收縮率和翹曲變形為評價指標，設計基於信噪比的正交試驗，利用灰色關聯分析法確定最優工藝參數組合，結果表明，優化後的兩個評價指標體積收縮率和翹曲變形分別降低了 22.27%，20.82%。再通過建立 EBF 神經網路模型結合 NSGA-II 多目標尋優演算法得到體積收縮率和翹曲變形的 Pareto 解集，最終確定最佳工藝參數為模具溫度 40.5°C，熔體溫度 221.4°C，注射時間 3.9 s，保壓壓力 54.8 MPa 及保壓時間 39.6 s，優化後製件體積收縮率最大為 5.475%，翹曲變形為 1.010mm。